



島根大学学術情報リポジトリ

S W A N

Shimane University Web Archives of kNowledge

Title

Cytotoxicity and pro-inflammatory effect of GaSb thin films in L929 cells

Author(s)

Fujihara J., Nishimoto N.

Journal

Int J Mod Phys B Vol. 35, No. 29, 2150297 (2021)

Published

2021

URL (The Version of Record)

<https://doi.org/10.1142/S0217979221502970>

この論文は出版社版ではありません。

引用の際には出版社版をご確認のうえご利用ください。

This version of the article has been accepted for publication,
but is not the Version of Record.

Cytotoxicity and pro-inflammatory effect of GaSb thin films in L929 cells

Junko Fujihara †

Department of Legal Medicine, Shimane University Faculty of Medicine, 89-1 Enya,

Izumo, Shimane 693-8501, Japan

jfujihar@med.shimane-u.ac.jp

Naoki Nishimoto

Department of Research Planning and Coordination, Shimane Institute for Industrial

Technology, 1 Hokuryo, Matsue, Shimane 690-0816, Japan

nishimoto.su2010@gmail.com

† Corresponding author.

Abstract

Gallium antimonide (GaSb)-based devices operate efficiently in the infrared region. Investigating the toxicity of GaSb thin film is necessary for using embedded GaSb-based devices in living organisms. In the present study, viability, oxidative stress, inflammatory responses, apoptosis induction, and genotoxicity of GaSb were assayed using L929 cells following a 24 h exposure to GaSb. GaSb thin films were deposited on a quartz substrate using RF magnetron sputtering. These films were soaked in cell culture medium to prepare test solutions. The viability of cells treated with the GaSb extract was lower than that of control cells. GaSb elicited little reactive oxygen species generation. Tumor necrosis factor- α and interleukin-1 β levels were elevated in GaSb-treated cell culture supernatants. Apoptosis and genotoxicity were not evident following GaSb treatment. Overall, these results demonstrate the low toxicity of GaSb compared with previous studies examining arsenic-containing III-V materials, which is desirable for biological devices.

Keywords GaSb; L929 cells; reactive oxygen species; pro-inflammatory response.

1. Introduction

The III-V compound semiconductors have been investigated as attractive materials for electronic devices.¹⁻³ The importance of III-V materials is increasing as they are applied to biological devices.^{4,5} Gallium antimonide (GaSb) is a III-V compound semiconductor with appealing physical properties that finds application in many fields. GaSb nanoparticles draw immense scientific interest because they can effectively form a bridge between bulk materials and atomic or molecular structures.⁶ Besides, GaSb has zinc-blende structure, and (111) of the structure has some similarities to the polycyclic aromatic hydrocarbons (PAH). Coronene (superbenzene) is one of the most popular PAH which has seven and six membered benzenoid rings has great attention for various electronic devices,^{7,8} Rubrene is a red PAH comprising a tetracene base with phenyl ring attached to both sides of two central benzene rings and rubrene-based device is applied to a radiation detector.⁹ Hence, PAH and GaSb can be compared on the physical side. On the other hand, because it has a relatively narrow band gap energy (0.73 eV at 300 K),¹⁰ the key applications of GaSb-based devices are infrared detectors, infrared LEDs, and infrared LDs.¹¹⁻¹³ In addition, GaSb has a high electron mobility and a high saturation velocity which are suitable for high-speed electronic devices.¹⁴ Thus, biomedical data can easily be obtained from biological materials by embedding GaSb-based devices such as an IR detector.¹⁵ In the case of biological applications, it is important that such implants do not elicit an

adverse reaction.

Ga and Sb are graded as harmful to humans and dangerous for the environment.¹⁶ Toxicities of III-V materials, such as gallium arsenide (GaAs) and indium arsenide (InAs), have been reported.^{17–21} However, there is a lack of available information on the toxicity of GaSb when compared to GaAs and InAs. We reported the characteristics of GaSb thin films grown by RF magnetron sputtering,²² and investigated the effect of surface coating on the biocompatibility and stability of GaSb thin films under simulated physiological conditions.¹⁵ In these previous studies, the *in vitro* cytotoxicities of GaSb thin films were not fully investigated. Therefore, investigating the toxicity of GaSb thin film is necessary for the use of embedded GaSb-based devices in a living body. In the present study, viability oxidative stress, inflammatory responses, apoptosis induction, and genotoxicity of GaSb thin films were examined using L929 cells.

2. Materials and Methods

2.1. Growth of GaSb thin films

According to our previous studies,^{15,22} GaSb thin films were grown on quartz substrates (10 × 10 mm, thickness 0.5 mm) by RF magnetron sputtering (HSR-351L, Shimadzu Industrial Systems, Otsu, Japan). The Ga content x in $\text{Ga}_x\text{Sb}_{1-x}$ was 0.6, and the film thickness was 200 nm.

2.2. Cytotoxicity assays

2.2.1. Cell culture

L929 cells (a mouse fibroblastic cell line) were provided by the RIKEN RBC through the National BioResource Project of the MEXT, Japan. RPMI 1640 medium containing 10% fetal bovine serum, 5 μ M 2-mercaptoethanol, and 10 U/mL penicillin was used for cell culture. Cells were cultured at 37°C, 5% CO₂, and > 95% humidity. L929 cells were plated into 96-well plates for 3-(4,5-Dimethylthiazol-2-yl)-2,5-diphenyltetrazolium bromide (MTT) assay and tumor necrosis factor (TNF)- α and interleukin (IL)-1 β measurement, were plated into 6-well plates for reactive oxygen species (ROS)/ superoxide detection, apoptosis assay, and Comet assay at a density of 5×10^3 cells/well.

2.2.2. MTT assay

Cell viability was assayed by using a MTT cell count kit (Nacalai Tesque, Kyoto, Japan). GaSb thin film was soaked in cell culture medium (20 mL) to prepare test solutions (24 h at 37°C). After 24 h of seeding cells, the culture medium was substituted by 100 μ L of the test solution or fresh culture medium (control), incubated for 24 h. The MTT solution (10 μ L) was added to each well and incubated for 4 h. The solution was removed, and the formazan crystal dissolving solution (100 μ L) was added. Absorbance measurements (570

nm: test, 690 nm: reference) were performed by a Multiskan™ GO microplate spectrophotometer (Thermo Fisher Scientific, Waltham, MA, USA).

2.2.3. ROS and superoxide detection

After seeding cells for 24 h, the culture medium was substituted by 1 mL of the test solution, fresh culture medium (control), or pyocyanin (positive control), and the 6 well culture plates were incubated for 1 h. Total ROS/Superoxide Detection Solution® (Enzo Life Sciences, Farmingdale, NY, USA) was added and the 6 well culture plates were incubated for a 30 min at 37°C. The cells were washed with wash buffer for three times, and fluorescent image was obtained with an EVOS FL fluorescence microscope cell imaging system (Thermo Fisher Scientific) with a filter cube for green fluorescent protein (GFP) and red fluorescent protein.

2.2.4. Measurements of TNF- α and IL-1 β

Following addition of the test solution, culture media were collected at days 1, 2, and 3, and the production of TNF- α and IL1- β was evaluated using enzyme-linked immunosorbent assay kits (R&D Systems, Minneapolis, MN, USA) in accordance with the manufacturer's instructions. Absorbance was measured at 450 nm with a Multiskan™ GO microplate spectrophotometer.

2.2.5. Apoptosis assay

After seeding cells on 6 well plate for 24 h, the culture medium was exchanged for the test solution or fresh culture medium (control). Following 1 h incubation, 100 μ L of the tetramethylrhodamine methyl ester (TMRE)/Hoechst dye staining solution (Cayman Chemical, Ann Arbor, MI, USA) were added to the plates. The supernatant was aspirated, and 2 mL of binding buffer was added to each well after 30 min incubation at 37°C. Next, 800 μ L of Annexin V solution was added to each well and the plates were incubated at room temperature for 10 min. The solution was discarded, and 2 mL of binding buffer were added. The cells were then imaged with an EVOS fluorescence microscope (Thermo Fisher Scientific) with a filter cube for GFP, 4', 6-diamidino-2-phenylindole, and red fluorescent protein.

2.2.6. Comet assay

As mentioned in apoptosis assay section, L929 cells were exposed to test solution. Then comet assay was performed using a COMET SCGE assay kit (Enzo Life Sciences). The cells were mixed with LMAgarose at a ratio of 1:10 and pipetted onto the Comet slide. Following immersion in alkaline solution, the Comet side was electrophoresed using a horizontal electrophoresis apparatus. The slide was stained with GREEN Dye and imaged

with an EVOS fluorescence microscope with a filter cube for GFP.

2.3. Ga and Sb measurements

Ga concentrations were determined by microwave plasma-atomic emission spectrometry (MP-AES; Agilent Technologies, Santa Clara, CA, USA) with an Inert One Neb nebulizer and a double-pass glass cyclonic spray chamber (Agilent Technologies). The total Sb concentration was measured by hydride generation-MP-AES using an MP-AES system connected to a multimode sample introduction system (Agilent Technologies) according to our previously reported method.²³

2.4. Statistical analyses

Data are represented as means \pm standard deviations. Between-control and treated group difference in cell viability was analyzed using Mann-Whitney unpaired test. Using Dunnett's test, the differences between control groups and treated groups in TNF- α and IL-1 β levels were analyzed.

3. Results

3.1. MTT assay

The cytotoxicity of extracts from the GaSb thin film, which was prepared by

soaking the films in culture medium, was assayed by the MTT assay. This assay measures reduction of the yellow MTT tetrazolium salt to purple formazan as a marker of metabolic activity (Fig. 1). Ga and Sb concentrations in the test solution were 1.40 and 1.77 $\mu\text{g/mL}$, respectively. The viability of cells treated with the GaSb extract was lower (67.7%) than that of control cells (100%).

3.2. ROS/superoxide detection

ROS and superoxide were detected by the total ROS/Superoxide Detection Solution and fluorescence imaging (Fig. 2). Cells stained green (ROS) or orange (superoxide) were slightly more abundant in cultures treated with GaSb. The present results suggest that little ROS was generated by GaSb exposure in L929 cells.

3.3. Pro-inflammatory response

TNF- α and IL-1 β are pro-inflammatory cytokines. TNF- α and IL-1 β levels in the supernatants of cell cultures treated with the GaSb test solution were investigated up to 3 days. Both TNF- α and IL-1 β levels significantly elevated at only day 3 when compared to the control group (Figs. 3A and 3B).

3.4. Apoptosis assay

Apoptosis caused by the GaSb extract was imaged with fluorescence microscopy

using Hoechst dye (which reveals nuclear morphology), TMRE (a dye whose intensity reflects the mitochondrial membrane potential), and FITC-conjugated Annexin V (which attaches to phosphatidylserine residues on the outer membrane of apoptotic cells) (Fig. 4). Hoechst dye staining showed that the nuclear morphology was not changed by GaSb exposure. With TMRE staining, we confirmed that GaSb-treated cells had the same membrane potential as control cells. Annexin V staining was negative in both control and GaSb-treated cells.

3.5. Comet assay

The Comet Assay, which is a single cell gel electrophoresis assay (SCGE), is a simple technique used for analyzing cellular DNA damage. DNA damage is assayed by measuring the displacement between the genetic material of the nucleus ('comet head') and the resulting 'tail'. Fluorescent images of the Comet assay are shown in Fig. 5. GaSb treatment showed similar images as the negative control: no tail was observed. This indicated that GaSb exposure has no effect on DNA damage.

4. Discussion

GaSb toxicity has not yet been thoroughly investigated. Because evaluating the semiconductor toxicity is important before biological application, we investigated the toxicity of GaSb thin films. To prepare the test solution, GaSb thin films were prepared and

immersed in culture medium. GaSb dissolved in this medium and Ga and Sb may have been present in the test solution as ions.

According to the MTT assay results, the viability of cells treated with the GaSb test solution for 24 h was lower than that of control cells (Fig. 1). One mechanism of this toxicity may be related to oxidative stress. In the present study, ROS and superoxide, common inducers of cell death,^{24,25} were observed with fluorescence imaging (Fig. 2). However, ROS and superoxide were only slightly more abundant in GaSb exposed cells compared to control cells. This result is in accord with our previous study using InSb.²⁶

Little information is available on ROS generation by III-V materials. Flora et al. reported that Ga treatment did not increase ROS and nitric oxide but GaAs and As treatment did (dose: 8, 15, 30 $\mu\text{g/mL}$).¹⁹ Verdugo et al. reported that the ROS generation was significantly increased by As but not by Sb exposure in HEK-293 cells at doses of 10 μM .²⁷ Jiang et al. reported that Sb_2O_3 caused a dose-dependent cytotoxicity and induced ROS resulting in increased cell apoptosis in HEK293 cells at 8 and 16 μM .²⁸ The dose of Ga was lower than that in previous studies, while that of Sb was similar to previous studies. The present study and previous studies indicated that GaSb induced little ROS when compared to As and Sb_2O_3 .

Previously, we reported that $\text{TNF-}\alpha$ and $\text{IL-1}\beta$ levels were elevated in mice treated intravenously with ZnO nanoparticles²⁹ and in L929 cells treated with these nanoparticles.³⁰

Reports on the pro-inflammatory effect of Ga and Sb are limited. Wolff et al. reported that significant cytotoxic, inflammatory, and fibrogenic responses occurred after 6 and 12 months after exposures of $23 \pm 5 \text{ mg/m}^3$ Ga_2O_3 particles by inhalation in F344 rats.³¹ In contrast, a recent study reported that Ga had anti-inflammatory activity and topical application of gallium maltolate at a concentration of 0.5% was observed to relieve pain.³² $\text{Ga}(\text{NO}_3)_3$ reduced the serum levels of $\text{TNF-}\alpha$, IL-6, and interferon- γ in mice at 7 mg/kg/day for 56 days.³³ Co-administration of glycyrrhizic acid and antimony gluconate induced pro-inflammatory cytokines in mice,³⁴ and meglumine antimoniate treatment up-regulated cytokine gene expression in dogs.³⁵ In the present study, $\text{TNF-}\alpha$ and IL-1 β levels were increased following exposure to GaSb for 3 days (Fig. 3). Thus, the pro-inflammatory effect of GaSb is relatively weak.

In this study, GaSb treatment did not induce apoptosis as shown by fluorescent imaging (Fig. 4). Flora et al. reported that the As moiety in GaAs was responsible for neuronal apoptosis in both *in vivo* and *in vitro* (dose: 8, 15, 30 $\mu\text{g/mL}$).¹⁹ Jiang et al. demonstrated Sb-induced apoptosis following exposure of HEK cells to Sb_2O_3 at 8 and 16 μM .²⁸ Previous studies indicated the genotoxicity of Sb as well as As,^{36,37} while Kuroda et al. reported that the pentavalent form of Sb did not show genotoxicity, in contrast to the trivalent form.³⁸ In the current study, the Comet assay indicated that GaSb treatment was not genotoxic (Fig. 5). Overall, these data show that exposure of GaSb may not induce

apoptosis and genotoxicity.

5. Conclusions

In this study, the toxicity of GaSb to L929 cells was investigated. GaSb induced little ROS generation, but a pro-inflammatory response was seen following 3 days of exposure. However, apoptosis and genotoxicity were not observed following GaSb treatment. These results demonstrate that the toxicity of GaSb is lower when compared to As-containing III-V materials. There is a possibility that GaSb may be applied for the embedding devices in living tissue such as a field-effect transistor-based biosensor (BioFET) by a simple method like coating.

Acknowledgments

This work was supported in part by JSPS KAKENHI grant number 17K19814 (Grants-in-Aid for Challenging Research (Exploratory)) to J. F. We would like to thank Editage (www.editage.com) for English language editing.

References

1. O. Ueda, *Microelectron. Reliab.* **39**, 1839 (1999).
2. I. Vurgaftman, J. R. Meyer, *J. Appl. Phys.* **89**, 5815 (2001).
3. M. Yamaguchi, *Phys. Status Solidi C* **12**, 489 (2015).
4. H. Li, Y. Xu, X. Li, Y. Chen, Y. Jiang, C. Zhang, B. Lu, J. Wang, Y. Ma, Y. Chen, Y. Huang, M. Ding, H. Su, G. Song, Y. Luo, X. Feng, *Adv. Healthcare Mater.* **6**, 1601013 (2017).
5. H. H. Jung, J. Song, S. Nie, H. N. Jung, M. S. Kim, J. W. Jeong, Y. M. Song, J. Song, K. I. Jang, *Adv. Mater. Technol.* **3**, 1800159 (2018).
6. H. Yasuda, H. Mori, *J. Nanomater.* **2011**, 90130 (2010).
7. D. Akay, E. Efil, N. Kaymak, E. Orhan, S. B. Ocak, *J. Radioanal. Nucl. Chem.* **318**, 1409 (2018).
8. D. Akay, U. Gökmen, S. B. Ocak, *Mater. Chem Phys.* **245**, 122708 (2020).
9. D. Akay, U. Gokmen, S. B. Ocak, *JOM* **72**, 2391 (2020).
10. P. S. Dutta, H. L. Bhat, V. Kumar, *J. Appl. Phys.* **81**, 5821 (1997).
11. A. Rogalski, P. Martyniuk, M. Kopytko, *Appl. Phys. Rev.* **4**, 031304 (2017).
12. Y. Zhou, Q. Lu, X. Chai, Z. Xu, J. Chen, A. Krier, L. He, *Appl. Phys. Lett.* **114**, 253507 (2019).
13. A. Joullié, P. Christol, *C. R. Physique* **4**, 621 (2003).
14. M. R. Tripathy, A. K. Singh, A. Samad, S. Chander, K. Baral, P. K. Singh, S. Jit, *IEEE Trans. Electron Devices* **67**, 1285 (2020).
15. N. Nishimoto, J. Fujihara, K. Yoshino, *Appl. Surf. Sci.* **409**, 375 (2017).
16. I. Cimboláková, I. Uher, K. V. Laktičová, M. Vargová, T. Kimáková, I. Papajová, in *Environmental Factors Affecting Human Health*, ed. Ivan Uher (IntechOpen, UK, 2020), p. 29.
17. M. T. Harrison, C. B. Hartmann, K. L. McCoy, *Toxicol. Appl. Pharmacol.* **186**, 18-27 (2003).
18. B. A. Fowler, E. A. Conner, H. Yamauchi, *Toxicol. Appl. Pharmacol.* **206**, 121 (2005).
19. S. J. Flora, K. Bhatt, A. Mehta, *Toxicol. Appl. Pharmacol.* **240**, 236 (2009).
20. S. J. Flora, K. Bhatt, N. Dwivedi, V. Pachauri, P. K. Kushwah, *Clin. Exp. Pharmacol. Physiol.* **38**, 423 (2011).
21. A. Tanaka, *Toxicol. Appl. Pharmacol.* **198**, 405 (2004).
22. N. Nishimoto, J. Fujihara, K. Yoshino, *J. Cryst. Growth* **468**, 732 (2017).
23. J. Fujihara, N. Nishimoto, *Microchemical Journal* **157**, 104992 (2020).
24. Y. Gong, X. D. Han, *Reprod. Toxicol.* **22**, 623 (2006).
25. H. Imai, Y. Nakagawa, *Free Radic. Biol. Med.* **34**, 145 (2003).
26. N. Nishimoto, J. Fujihara, *Int. J. Mod. Phys. B* **33**, 1950109 (2019).
27. M. Verdugo, Y. Ogra, W. Quiroz, *J. Toxicol. Sci.* **41**, 783 (2016).
28. X. Jiang, Z. An, C. Lu, Y. Chen, E. Du, S. Qi, K. Yang, Z. Zhang, Y. Xu, *Toxicol. Lett.* **256**, 11 (2016).
29. J. Fujihara, M. Tongu, H. Hashimoto, Y. Fujita, N. Nishimoto, T. Yasuda, H. Takeshita, *Eur. Rev. Med. Pharmacol. Sci.* **19**, 4920 (2015).
30. J. Fujihara, H. Hashimoto, N. Nishimoto, M. Tongu, Y. Fujita, *Surf. Rev. Lett.* **25**, 1850084 (2018).
31. R. K. Wolff, R. F. Henderson, A. F. Eidson, J. A. Pickrell, S. J. Rothenberg, F. F. Hahn, *J. Appl. Toxicol.* **8**, 191 (1988).
32. L. R. Bernstein, *Pain Med.* **13**, 915 (2012).
33. J. H. Choi, J. H. Lee, k. H. Roh, S. K. Seo, I. W. Choi, S. G. Park, J. G. Lim, W. J. Lee, M. H. Kim, K. R. Cho, Y. J. Kim, *Int. Immunopharmacol.* **20**, 269 (2014).
34. A. Bhattacharjee, S. Majumder, S. B. Majumdar, S. K. Choudhuri, S. Roy, S. Majumdar, *Int. J. Antimicrob. Agents* **45**, 268 (2015).
35. M. F. Santos, G. Alexandre-Pires, M. A. Pereira, L. Gomes, A. V. Rodrigues, A. Basso, A. Reisinho, J. Meireles, G. M. Santos-Gomes, I. P. da Fonseca, *Front. Vet. Sci.* **6**, 362 (2019).
36. T. Gebel, *Chem. Biol. Interact.* **107**, 131 (1997).
37. K. Asakura, H. Satoh, M. Chiba, M. Okamoto, K. Serizawa, M. Nakano, K. Omae, *J. Occup. Health* **51**, 498 (2009).
38. K. Kuroda, G. Endo, A. Okamoto, Y. S. Yoo, S. Horiguchi, *Mutat. Res.* **264**, 163 (1991).

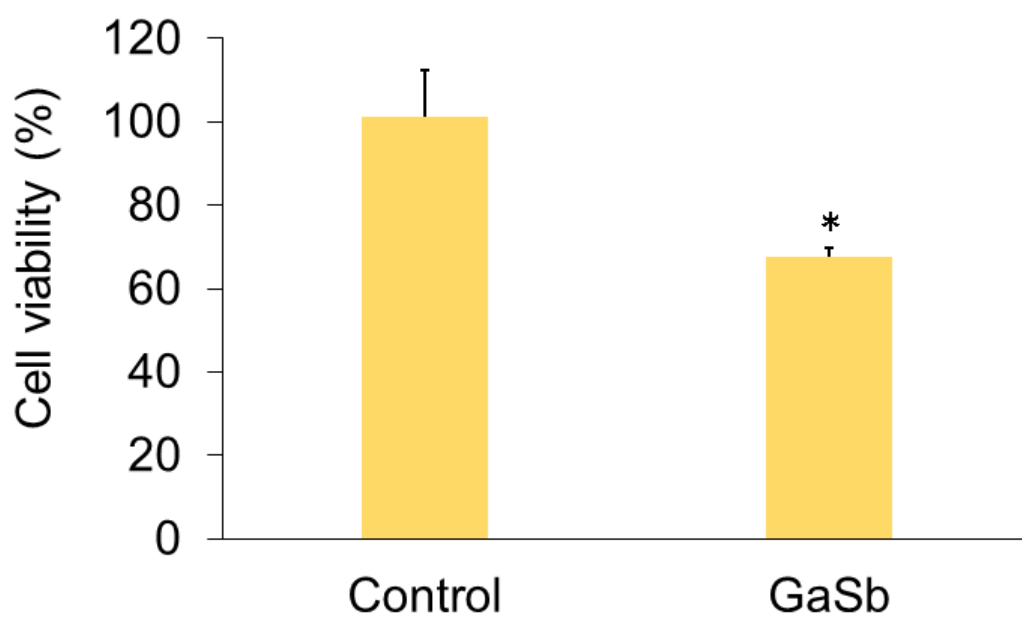


Fig. 1. Cell viability of L929 cells assayed by the MTT assay. After adding the GaSb test solution to each well, the cells were incubated for 24 h. Controls were assayed without the thin film test solution. Each value is the mean \pm standard deviation of three experiments. * $p < 0.05$ vs. the control group.

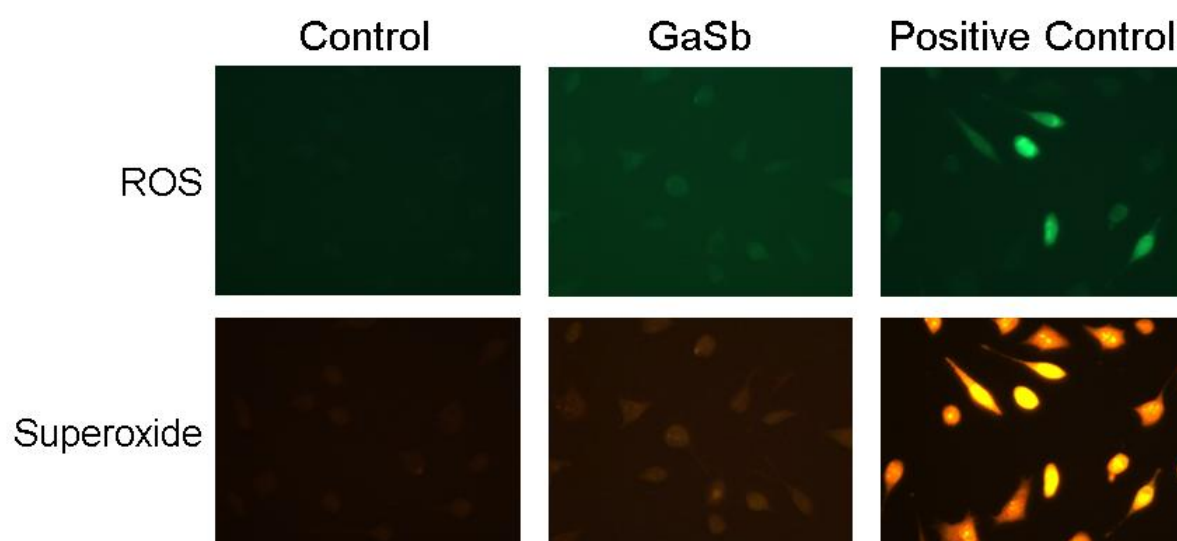


Fig. 2. Fluorescent images of L929 cells following 24 h exposure to GaSb. Orange (top) and green (bottom) in the fluorescent images display reactive oxygen species (ROS) and superoxide, respectively.

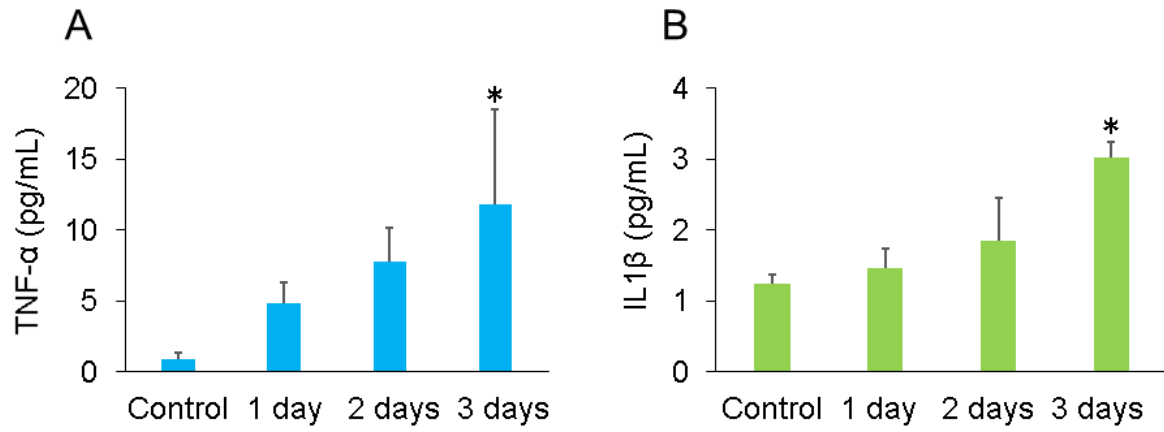


Fig. 3. Tumor necrosis factor (TNF)- α (A) and interleukin (IL)-1 β (B) levels in supernatants of L929 cultures following a 24 h treatment with GaSb. Values are the means \pm standard deviation of six experiments. * $p < 0.05$ vs. the control group.

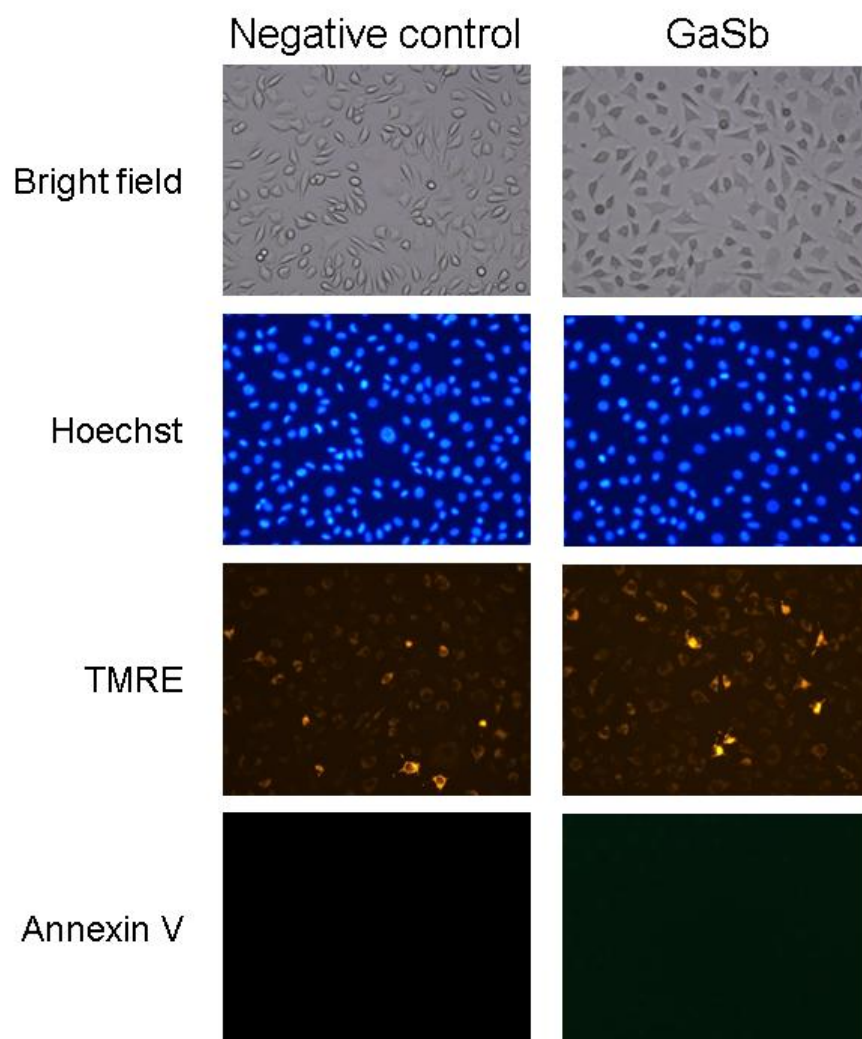


Fig. 4. Images of L929 cells following exposure to GaSb. The top images are bright field. The second row are nuclear Hoechst-stained fluorescent images. The third row are TMRE-stained fluorescent images representative of the mitochondrial membrane potential. The bottom images show fluorescent Annexin V staining.

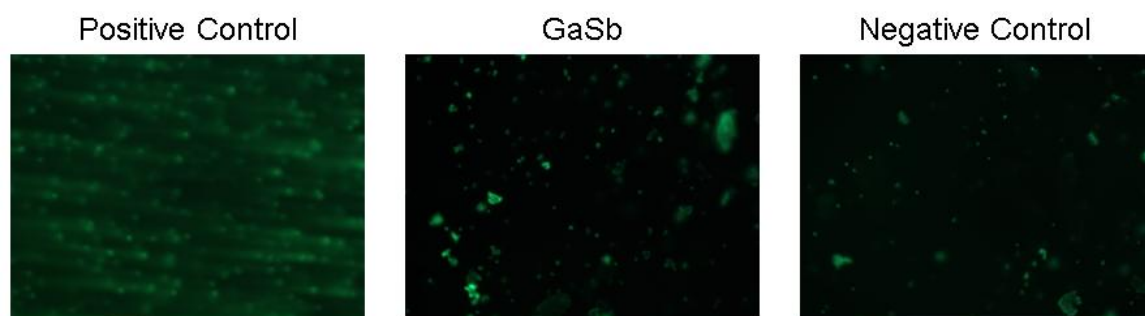


Fig. 5. Fluorescent images of the Comet assay in L929 cells treated with GaSb.